Neural network approach to the quantitative analysis of low-resolution gamma spectra with uncertainty

Jinhwan Kim, Kilyoung Ko, Wooseub Kim, Gyuseong Cho*
Department of Nuclear & Quantum Engineering, Korea Advanced Institute of Science and Technology, Republic of Korea
*Corresponding author: gscho@kaist.ac.kr

1. Introduction

The aim of radioisotope (RI) identification algorithms is to identify or quantify radioactive materials by measuring the energy of the emitted gamma rays. Various fields such as homeland security, decontamination, nuclear nonproliferation, radioactive waste, and many other disciplines that involve radiation rely on various types of detectors combined with algorithms to detect nuclear threats, track and investigate radioactive materials. The ideal detector used for these purposes typically requires the following physical properties: high-energy resolution, temperature-independent gain shift, high detection efficiency, and a large variety of shapes. So far, none of the detector types has met all of these conditions; while a high purity germanium (HPGe) detector has high energy resolution but fall short of other conditions, a thallium sodium iodide (NaI (Tl)) detector is high efficient in detection and varies in shape, but does not meet other requirements. The high-energy resolution and temperature-independent gain shift are the properties to facilitate the RI identification. If the results of the RI analysis with spectra obtained from the NaI(Tl) detector with these properties are comparable to those of the HPGe detector with good resolution, the NaI(Tl) detector might be an appealing choice close to the ideal detector. In this regard, various RI identification algorithms have been proposed to overcome the physical limitations of the NaI(Tl) detector. Although many of the algorithms have shown their effectiveness in analyzing RIs, it seems necessary to improve the accuracy of RI analysis for the low-resolution spectra.

In this paper, we proposed an ANN-based algorithm that automatically analyzes gamma-ray spectra and provides the all identified radioisotopes (RIs) with their fractional activities. The performance of the proposed algorithm was verified as follows: (1) the algorithm was applied both to the spectra obtained by the NaI(Tl) and HPGe detectors, and the results were compared; (2) spectra shifted to the maximum by the temperature change from 0 to 50 ℃ were evaluated. To accurately evaluate the algorithms with fractional activities of RIs, the following certified reference material was used: ^{152}Eu ,^{154}Eu ,^{22}Na, ^{54}Mn, ^{57}Co, ^{60}Co, ^{109}Cd, ^{133}Ba, and ^{137}Cs.

2. Methods and Results

2.1 Training and validation sets creation

The performance of the ANN-based algorithm depends largely on what data is used for training. In addition, large data is required to prevent overfitting. To this end, Monte-Carlo simulation was used to produce various spectral shapes by mimicking measured spectra [1–3]. However, the accuracy of predicted results tended to be degraded when evaluating measured spectra due to a discrepancy between measured and simulated spectra [2,3]. Instead, we synthesized the various shapes of spectra (synthetic spectra) by assuming the measured spectrum could be considered as a linear combination of base spectra, described as

$$S = \sum_{i=1}^{I} \epsilon_{int,i} g_i r_i B_i \quad (1)$$

where S denotes the estimated spectrum, I is the population of RIs, $\epsilon_{int,i}$ represents intrinsic efficiency, g_i is gamma yield, r_i is the relative activities of the RIs, and B_i represents the base spectrum for RI i retrieved from a spectra library. The number of the target RIs and the output nodes of the ANN should be the same. As shown in Fig.1 the synthetic spectrum better mimics the measured spectrum than the spectrum simulated by Monte Carlo N-Particle Transport Code 6 (MCNP6).

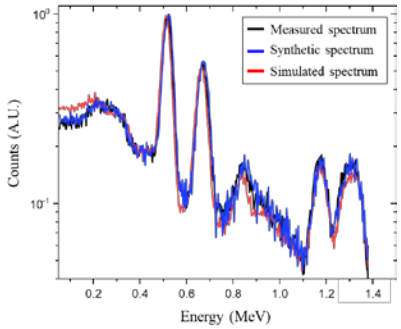

Fig. 1. A comparison of measured, simulated, and synthetic spectra. Their relative activity ratios were ^{137}Cs 39.0, ^{22}Na 30.5, ^{60}Co 23.5 and ^{54}Mn 7.0%

In addition, this synthetic spectrum can be easily generated in large amounts of data. The detail process of synthesizing spectra is as follows. The specific RIs were chosen from the base spectra library. The number of selected RIs was randomly selected ranging 1-5. Their relative activities corresponding to the selected

RIs was randomly sampled while others assigned zero. Then, the synthetic spectrum was made according to (1), where the intrinsic efficiency of the RIs was calculated by MCNP6. To mimic shifted spectra due to the gain shift effects, each channel in the spectrum was linearly repositioned. The shifted spectrum was reconstructed using spline interpolation with the original channels. The magnitude of this shift was randomly selected between 0.92 and 1.05. This shifted spectrum does not reflect the features of the actual measured spectrum, such as electrical noise and uncertainty. To mimic a more realistic spectrum, white noise was added to the spectrum. Then, the spectrum was normalized. This process was repeated to generate 500,000 and 5,000 spectra for training and validation sets, respectively.

2.2 Test set creation

To create the test set, the gamma spectra were measured with five different combinations of RIs, as presented in Table 1.

Table 1. Five different combinations of RIs and their relative activity ratios

Case	RI	Ratio (%)
1	^{152}Eu	100
2	^{57}Co	31.1±0.9
	^{109}Cd	68.9±2.0
3	^{152}Eu	26.3±0.8
	^{154}Eu	25.0±0.8
	^{60}Co	21.4±0.6
	^{137}Co	27.3±0.8
4	^{152}Eu	22.6±0.7
	^{154}Eu	21.5±0.6
	^{60}Co	18.4±0.6
	^{137}Cs	23.4±0.7
	^{22}Na	14.1±0.4
5	^{152}Eu	21.7±0.7
	^{154}Eu	20.7±0.6
	^{137}Cs	22.5±0.7
	^{54}Mn	3.9±0.1
	^{60}Co	17.6±0.5
	^{22}Na	13.6±0.4

The corresponding CRMs were placed 6cm away from the NaI(Tl) or HPGe detectors for 300 seconds at room temperature 20℃. Two more test sets were made by assuming gain shift and uncertainty scenarios. The gain shift scenario was intended to ensure that accuracy is maintained when the spectra shift due to temperature changes. The spectra were measured under the same conditions as above, but the temperature was changed to 50℃ where the spectrum was shifted the most in the negative direction. This temperature was determined by ascertaining the extent to which the ^{60}Co spectrum shifted while adjusting the temperatures of 0-50 ℃ in steps of 5 ℃ (Fig. 2). In each step, the temperature was held for 2 hours to achieve temperature equilibrium in the entire volume of the scintillator. It should be noted that the NaI(Tl) detector connected with the PMT was placed in the constant-temperature oven (HG-THC150), while the others such as an amplifier (ORTEC 673) and a mulita channel analyzer (ORTEC TRUMP-PCI-2k) were placed outside of the oven at constant room temperature. In this figure, the spectrum shifted little in the positive direction. This might be because the light yield of the NaI(Tl) scintillators tends to slightly increase and decrease as the temperature increases, while the PMT gain tends to decrease [4]. Though the spectrum was rarely shifted in this case, the spectra were intentionally biased to the positive direction by adjusting the gain and measured for the gain shift scenario. The uncertainty scenario was intended to evaluate how well the proposed algorithm analyzes high uncertainty spectra without obvious photo-peaks. For this, the acquisition time was reduced from 60 to 0.1 s with intervals of 5 or 1 or 0.1 s, and the spectrum was measured 10 times at each times.

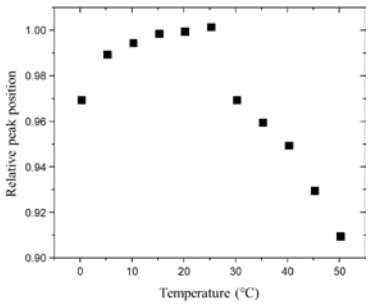

Fig. 2. Relative ^{60}Co peak position versus temperature change of 0-50 ℃

2.3 Hyper-parameter optimization

The proposed ANN has several hyper-parameters: the number of layers, the number of neurons and the activation function in each layer, the learning rate of the Adam optimizer, and the neuron dropout rate. Choosing the optimal hyper-parameters is a crucial task because it can have a significant impact on the performance of the ANN. Softmax activation function in the last layer was used to quantify the probability liked to each output neuron. Although this function is traditionally used for classification, it showed its effectiveness in a regression model [1]. The remaining hyper-parameters were determined using Bayesian optimization which uses all information available from previous evaluations of the model to decide where to sample for the next evaluation, whereas the grid search and random search methods are independent of the previous run [5,6]. Bayesian optimization consists of two main parts. It builds a statistical model f, which is a Gaussian process due to its flexibility and tractability for the objective function, in this case the cross-entropy function, and updates the posterior probability distribution on f using all available data. The mean and covariance matrix for the

posterior distribution were calculated using the Matern 5/2 kernel function [5]. Then, the acquisition function is calculated using the current posterior distribution. Here, the expectation improvement was used to determine the next sampling point to evaluate. We used Bayesian optimization as implemented in the Python package GpyOpt version 1.2.0, searching the space of the hyper-parameters listed in Table 3. The optimized hyper-parameters in the search space were also shown in Table 3. Training was terminated when there was no decrease in the mean cross entropy error of the validation set during 100 consecutive epochs.

3. Result and discussion

In order to validate the performance of the proposed algorithm with regard to the quantitative analysis of RIs, we quantify the fractional activities of RIs contributing to the spectra measured both by the NaI(Tl) and HPGe detectors for the five cases (Table 1). To directly compare the results, the error was defined, shown as

$$\text{error}\ (\%) = 100\sqrt{\sum_{n=1}^{N}(y_n - \hat{y}_n)^2} \quad (2)$$

where y_i is the truth of ith output, and $\hat{y}_i$ is the ANN output of the ith output. An example of comparison results is shown in Fig. 3 and Table 2. It was confirmed that the proposed algorithm is able to estimate the relative activity of the identified RIs contributing the spectra measured by both the NaI(Tl) and HPGe detectors.

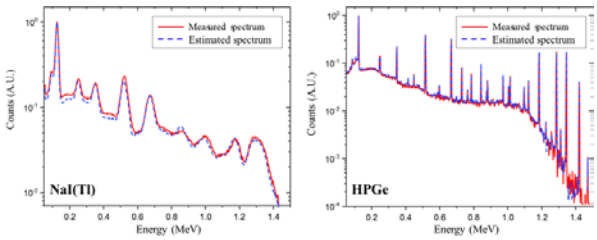

Fig. 3. Measured spectrum of the case 5 (^{152}Eu, ^{154}Eu, ^{60}Co, ^{137}Cs, ^{22}Na, ^{54}Mn) against the estimated by ANN-based algorithm

Table 2. Comparison results of quantitative analysis of the NaI(Tl) and HPGe spectra for the case 5

RIs	True(%)	Predict(%)	
		NaI(Tl)	HPGe
^{152}Eu	21.7	21.2	19.8
^{154}Eu	20.2	20.7	19.1
^{137}Cs	22.5	21.9	21.8
^{54}Mn	3.9	6.4	5.9
^{60}Co	17.6	18.3	20.5
^{22}Na	13.6	10.7	12.9
Error (%)		4.0	4.3

Fig. 4 also shows the case 5 spectra shifted in the positive and negative directions. The errors with the negative and positive directions were 4.3 and 5.5%, respectively, which demonstrate only very slight increases. This is because the training data was made considering shifted spectra so that the positional effects on features such as the photo-peak are minimized and overall spectral shape was trained. Note that these spectra would be difficult to analyze without recalibration.

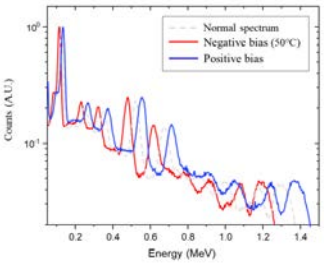

RIs	True(%)	Predict(%)	
		Positive	Negative
^{152}Eu	21.7	20.5	17.8
^{154}Eu	20.2	19.6	20.0
^{137}Cs	22.5	22.5	21.6
^{54}Mn	3.9	5.5	7.0
^{60}Co	17.6	18.1	19.7
^{22}Na	13.6	9.9	13.5
Error (%)		4.3	5.5

Fig. 4. Case 5 spectra measured at temperature 20 and 50 ℃, and the spectrum positively baised by adjusting the gain

To investigate how well the ANN analyzes high uncertainty spectra without obvious photo-peaks, the spectra were measured while reducing the acquisition time. As presented in Fig. 5(a), as the acquisition time increases, errors and deviations tend to decrease for the case 4. In particular, the error is significantly reduced after 2 s measurement. This tendency was similar in other cases. Figure 5(b) shows the case 4 spectrum measured for 2 s and the estimated spectrum based on the determined relative activities of the identified RIs. Despite a lack of obvious photo-peaks, the well trained ANN identified RIs and determined their relative activities. This is because when synthesizing spectra for the training data, various magnitudes of white noise were added to mimic actual measured spectra with short acquisition time.

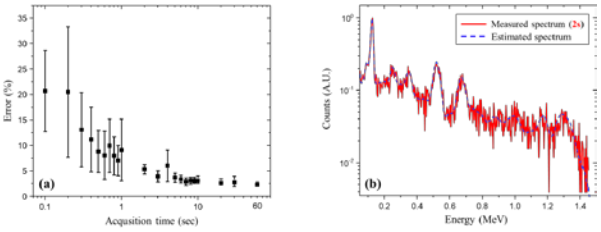

Fig. 5. (a) Error changes with increasing acquisition time (b) 2 sec measured spectrum for the case 4 (^{152}Eu, ^{154}Eu, ^{60}Co, ^{137}Cs, ^{22}Na) against the estimated by ANN-based algorithm

4. Conclusion

We have described an ANN-based algorithm that automatically analyzes low-resolution NaI(Tl) spectra

and determines the fractional activities of all the identified RIs. It was confirmed that the low-resolution spectra can be quantitatively analyzed as precisely as the results of the HPGe spectra at the possible exposure temperature changes of 0-50 ℃. Furthermore, high uncertainty spectra can be analyzed with precision. These results show the possibility of using the NaI(Tl) detector as the ideal-like detector by overcoming its physical limitations such as low-resolution and temperature-dependence gain shift using the proposed ANN-based algorithm.

REFERENCES

[1] M. Kamuda, J. Stinnett, C.J. Sullivan, Automated Isotope Identification Algorithm Using Artificial Neural Networks, IEEE Trans. Nucl. Sci. 64 (2017) 1858–1864. doi:10.1109/TNS.2017.2693152.

[2] J. Kim, K. Park, G. Cho, Multi-radioisotope identification algorithm using an artificial neural network for plastic gamma spectra, Appl. Radiat. Isot. 147 (2019) 83–90. doi:10.1016/j.apradiso.2019.01.005.

[3] L.J. Kangas, P.E. Keller, E.R. Siciliano, R.T. Kouzes, J.H. Ely, The use of artificial neural networks in PVT-based radiation portal monitors, Nucl. Instruments Methods Phys. Res. A. 587 (2008) 398–412. doi:10.1016/j.nima.2008.01.065.

[4] Z.M. Wang, Y.H. Yu, Z.Y. Sun, K. Yue, D. Yan, Y.J. Zhang, Y. Zhou, F. Fang, W.X. Huang, J.L. Chen, Temperature dependence of the plastic scintillator detector for DAMPE, Chinese Phys. C. 41 (2017) 3–9. doi:10.1088/1674-1137/41/1/016001.

[5] J. Snoek, H. Larochelle, R.P. Adams, Practical Bayesian Optimization of Machine Learning Algorithms, NIPS Proc. (2012) 1–9. doi:2012arXiv1206.2944S.

[6] J. Bergstra, Y. Bengio, Random Search for Hyper-Parameter Optimization, J. Mach. Learn. Res. 13 (2012) 281–305. doi:10.1162/153244303322533223.